Direct Adaptive Inverse Control via Modified Variable Step Size FLMS Algorithm

Rodrigo Possidônio Noronha
Department of Electrical Engineering
Federal Institute of Education, Science and Technology of Maranhão
Imperatriz, Brazil
rodrigo.noronha@ifma.edu.br

***Abstract*—This work proposes a new methodology of Direct Adaptive Inverse Control (DAIC) via Modified Variable Step Size Fractional Least Mean Square (MVSS-FLMS) algorithm. The main objective of this work is to analyze the performance of MVSS-FLMS algorithm in DAIC design, in terms of convergence speed of the controller weight vector and steady-state Mean Square Error (MSE) of the error used to update the estimate of the controller weight vector. The results obtained in DAIC design through MVSS-FLMS algorithm were compared with the results obtained through Fractional Least Mean Square (FLMS) algorithm. As a complexity scenario, the proposed methodology was evaluated on a non-minimum phase plant in the presence of a disturbance signal added to the control signal. In addition, the reference signal used is of sinusoidal type.**

***Index Terms*—Adaptive Inverse Control, Fractional LMS, Inverse Model, FIR Filter, Non-minimum Phase.**

I. Introduction

Since Adaptive Inverse Control (AIC) was proposed by [1], several contributions to this method have been proposed in the literature [2]–[8]. A promising contribution to AIC theory was proposed by [9] and titled Direct Adaptive Inverse Control (DAIC). Like AIC, DAIC is a control technique based on plant model inverse identification, such that in the absence of uncertainty, the controller is equal to the plant inverse model. For DAIC, due to the controller weight vector to be updated as a function of the reference error and to be implemented in a quasi-feedforward configuration, the controller is designed to track the plant inverse dynamics even in the presence of disturbance signals. Several contributions to DAIC theory have been proposed in the literature. In [10], neural DAIC based on nonlinear model identification was proposed. In [11], a DAIC methodology was proposed for position and speed control of electric motors. In [12], a neural DAIC methodology for Skid Steering boat control was proposed.

In this work, the controller is represented by a Finite Impulse Response (FIR) type adaptive filter. Since the controller is defined by a linear mathematical representation, then it is possible to use algorithms based on stochastic gradient to estimate the controller weight vector [11]. In the literature, the controller weight vector of DAIC has generally been estimated using the following algorithms based on stochastic gradient: Least Mean Square (LMS) [13] and Normalized Least Mean Square (NLMS) [11].

The development of methodologies for fractional signal processing based on the theory of fractional calculus is of great interest to scientific community of mathematics, physics and engineering [14]. The fractional calculus was proposed in the late 17th century by Liouville, Reimann and Leibniz [15] and, is a generalization of the traditional calculus, such that the order of derivation and integration operations is a fractional number [16]. Fractional calculus is used to model dynamics systems of different natures, such as Brownian motion, diffusion systems, harmonic oscillators, and others [17]. Other applications can be seen, for example, in control system [18], [19], neural networks [20], identification systems [21]–[23], time series prediction [24], [25], classification [26] and optimization [27]. In the context of adaptive algorithms based on stochastic gradient, in [28] a new version of LMS algorithm based on the Rieman-Liouville fractional derivative definitions was proposed, titled Fractional Least Mean Square (FLMS). In this present paper, the estimation of the weight vector of DAIC was performed through the Modified Variable Step Size FLMS (MVSS-FLMS) algorithm, proposed in [29]. The MVSS-FLMS algorithm is an improvement of FLMS, such that the adjustment of the step size is performed with the goal of obtaining a good trade-off between the convergence speed and the steady-state Mean Square Error (MSE) [29].

The main contribution of this work is to evaluate the performance of MVSS-FLMS algorithm in DAIC design, in terms of convergence speed of the controller weight vector and steady-state MSE. In addition, the results obtained in DAIC design through MVSS-FLMS algorithm were compared with the results obtained through FLMS algorithm. Until the present moment, according to the bibliographical studies carried out by the author of this paper, no contribution to the DAIC design has been proposed using the MVSS-FLMS algorithm. The performance analysis was performed on a non-minimum phase plant in the presence of a periodic disturbance signal added to the control signal. This paper is organized with the following sections: in Section II, the mathematical formulations for DAIC are presented; in Section III, the mathematical formulations of MVSS-FLMS algorithm are presented; in Section IV, the computational results obtained are presented.

Notation: Matrices and vectors are denoted by bold letters. The superscripts $(\bullet)^{\mathrm{T}}$ represent a transposed matrix. The operator $\mathrm{E}[\bullet]$ represents the expected value of a aleatory variable.

II. Direct Adaptive Inverse Control

In this work, the plant model $P(q^{-1})$ in discrete time is considered monovariable, stable, causal, and non-minimum phase, such that the relationship between the plant output signal $y(k)$ and the control signal $u(k)$ is given by:

$$y(k) = q^{-d}\frac{B(q^{-1})}{A(q^{-1})}u(k) = P(q^{-1})u(k), \tag{1}$$

where $A(q^{-1}) = 1 + a_1q^{-1} + a_2q^{-2} + \ldots + a_nq^{-n}$ and $B(q^{-1}) = 1 + b_1q^{-1} + b_2q^{-2} + \ldots + b_mq^{-m}$ with $n, m \in \mathbb{N}$. It is important to note that (1) is described as a function of the N-th delay operator q^{-N}, which performs the following operation $q^{-N}r(k) = r(k-N)$ with $N \in \mathbb{N}$ and $k \in \mathbb{N}$ represents the k-th time instant. In addition, $d \in \mathbb{N}$ is the delay size between $u(k)$ and $y(k)$. In this work, the control configuration used for the DAIC is shown in Fig. 1 [11].

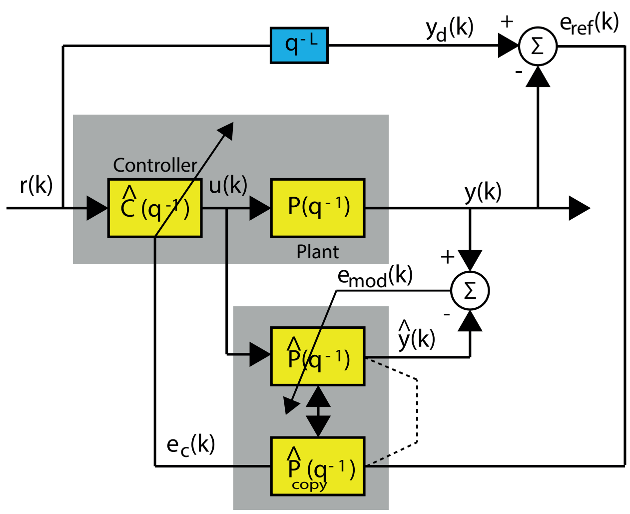

Fig. 1: Block diagram for the DAIC.

As proposed by [11], in the DAIC configuration shown in Fig. 1, the controller, estimated directly as a function of the reference error $e_{ref}(k)$ and error estimation $e_{mod}(k)$, is represented by $\hat{C}(q^{-1})$. It is important to note that in the absence of uncertainty the controller $\hat{C}(q^{-1})$ is equal to the plant inverse model. In addition, a delay block is inserted between the reference signal $r(k)$ and the signal $y_d(k)$, such that $q^{-L}r(k) = r(k-L) = y_d(k)$, where $L \cong (\mathcal{M}+d+m)/2$ and $\mathcal{M}$ is the generic order of the controller [11].

In this work, the controller is represented by an M-order adaptive FIR filter, where $\mathbf{\Theta}(k) \in \mathbb{R}^{M\times 1}$ is the weight vector. The control signal $u(k)$ is given by:

$$u(k) = \hat{C}(q^{-1})r(k), \tag{2}$$

which can be rewritten as follows:

$$u(k) = \theta_0 r(k) + \theta_1 r(k-1) + \ldots + \theta_{M-1}r(k-M+1), \tag{3}$$

since $\hat{C}(q^{-1}) = \theta_0 + \theta_1 q^{-1} + \theta_2 q^{-2} + \ldots + \theta_{M-1}q^{-M+1}$. In compact form, (3) is rewritten in vector notation, given by:

$$u(k) = \mathbf{\Psi}^{\mathrm{T}}(k)\mathbf{\Theta}(k) = \mathbf{\Theta}^{\mathrm{T}}(k)\mathbf{\Psi}(k), \tag{4}$$

where $\mathbf{R}(k) = [r(k)\ r(k-1)\ \ldots\ r(k-M+1)]^{\mathrm{T}} \in \mathbb{R}^{M\times 1}$ is the reference signal vector.

The update of the estimate of the weight vector $\mathbf{\Theta}(k)$ is given as a function of the error $e_c(k)$. It is important to note that the update of the error $e_c(k)$ is given as a function of the update of the estimated plant model $\hat{P}(q^{-1})$. In this work, $\hat{P}(q^{-1})$ is represented by an N-order adaptive FIR filter, where $\mathbf{\Pi}(k) \in \mathbb{R}^{N\times 1}$ is the weight vector. The output signal $\hat{y}(k)$ of $\hat{P}(q^{-1})$ is given by:

$$\hat{y}(k) = \hat{P}(q^{-1})u(k), \tag{5}$$

which can be rewritten as follows:

$$\hat{y}(k) = \pi_0 u(k) + \pi_1 u(k-1) + \ldots + \pi_{N-1}u(k-N+1), \tag{6}$$

since $\hat{P}(q^{-1}) = \pi_0 + \pi_1 q^{-1} + \pi_2 q^{-2} + \ldots + \pi_{N-1}q^{-N+1}$. In compact form, (6) is rewritten in vector notation, given by:

$$\hat{y}(k) = \boldsymbol{\mathcal{U}}^{\mathrm{T}}(k)\mathbf{\Pi}(k) = \mathbf{\Pi}^{\mathrm{T}}(k)\boldsymbol{\mathcal{U}}(k), \tag{7}$$

where $\boldsymbol{\mathcal{U}}(k) = [u(k)\ u(k-1)\ \ldots\ u(k-N+1)]^{\mathrm{T}} \in \mathbb{R}^{N\times 1}$ is the control signal vector.

It is important to note that the update of the estimate of the weight vector $\mathbf{\Pi}(k)$ of $\hat{P}(q^{-1})$ is given as a function of estimation error $e_{mod}(k)$. The estimation error $e_{mod}(k)$ is given by:

$$e_{mod}(k) = y(k) - \hat{y}(k) = \left[P(q^{-1}) - \hat{P}(q^{-1})\right]u(k) \tag{8}$$

After this, the error $e_c(k)$ needed to update the estimate of the weight vector $\mathbf{\Theta}(k)$ of $\mathbf{C}(q^{-1})$ is obtained. The error $e_c(k)$ is given by:

$$e_c(k) = \hat{P}(q^{-1})e_{ref}(k), \tag{9}$$

which is equivalent to following difference equation $e_c(k) = \pi_0 e_{ref}(k) + \pi_1 e_{ref}(k-1) + \ldots + \pi_{N-1}e_{ref}(k-N+1)$, where $e_{ref}(k)$, which is the reference error, is given by:

$$\begin{aligned} e_{ref}(k) &= q^{-L}r(k) - y(k) \\ &= r(k-L) - y(k) \\ &= y_d(k) - y(k) \end{aligned} \tag{10}$$

III. Modified Variable Step Size FLMS Algorithm

Let $\mathbf{\Upsilon}(k) \in \mathbb{R}^{M\times 1}$ be the weight vector of an adaptive FIR filter. According to Wiener criterion [30], the update of the estimate of the weight vector of an adaptive FIR filter is obtained as follows:

$$\mathbf{\Upsilon}(k+1) = \mathbf{\Upsilon}(k) - \frac{1}{2}\mu\nabla_{\mathbf{\Upsilon}(k)}(\mathrm{E}[e^2(k)]), \tag{11}$$

where the cost functional $J = \nabla_{\mathbf{\Upsilon}(k)}(\mathrm{E}[e^2(k)])$ is given as a function of the stochastic gradient of the squared error $e^2(k) = (\bar{d}(k) - \hat{d}(k))^2$ with $\hat{d}(k) = \mathbf{\Upsilon}^{\mathrm{T}}(k)\boldsymbol{\mathcal{X}}(k) = \boldsymbol{\mathcal{X}}^{\mathrm{T}}(k)\mathbf{\Upsilon}(k)$. It is important to note that μ is the step size, $\bar{d}(k)$ is the system output signal and $\hat{d}(k)$ is the output signal of the adaptive

FIR filter. The goal of Wiener criterion is the minimization of $\nabla_{\mathbf{\Upsilon}(k)}(\mathrm{E}[e^2(k)])$, where the optimal solution is given by $\mathbf{\Upsilon}_0 = \mathbf{R}^{-1}\mathbf{p}$ with $\nabla_{\mathbf{\Upsilon}(k)}(\mathrm{E}[e^2(k)]) = 2\mathbf{R}\mathbf{\Upsilon}(k) - 2\mathbf{p}$, where $\mathbf{R} = \mathrm{E}[\boldsymbol{\mathcal{X}}(k)\boldsymbol{\mathcal{X}}^{\mathrm{T}}(k)]$ is the autocorrelation matrix and $\mathbf{p} = \mathrm{E}[\boldsymbol{\mathcal{X}}(k)d(k)]$ is the cross-correlation vector. It is quite costly, in the context of real-time operation, to work with the autocorrelation matrix and cross-correlation vector to obtain the optimal solution $\mathbf{\Upsilon}_0$. This problem can be solved by reformulating the cost functional as a function of the instantaneous values of the squared error. Thus, the cost functional J is rewritten as follows:

$$J = \nabla_{\mathbf{\Upsilon}(k)}(e^2(k)), \tag{12}$$

substituting (12) into (11), it is obtained the LMS algorithm, given by:

$$\begin{aligned} \mathbf{\Upsilon}(k+1) &= \mathbf{\Upsilon}(k) - \frac{1}{2}\mu\nabla_{\mathbf{\Upsilon}(k)}(e^2(k)) \\ &= \mathbf{\Upsilon}(k) + \mu e(k)\boldsymbol{\mathcal{X}}(k), \end{aligned} \tag{13}$$

where $\nabla_{\mathbf{\Upsilon}(k)}(e^2(k)) = -2e(k)\boldsymbol{\mathcal{X}}(k)$.

Using the FLMS algorithm, the weight vector of the adaptive FIR filter can be updated as follows [28]:

$$\mathbf{\Upsilon}(k+1) = \mathbf{\Upsilon}(k) - \mu\frac{\partial J(k)}{\partial\mathbf{\Upsilon}(k)} - \mu_f\left(\frac{\partial J(k)}{\partial\mathbf{\Upsilon}(k)}\right)^v J(k), \tag{14}$$

where $v \in (0,1)$ is the fractional order of the derivative [14].

Through the chain rule, the partial derivative $\dfrac{\partial J(k)}{\partial\mathbf{\Upsilon}(k)}$ is given by [31]:

$$\frac{\partial J(k)}{\partial\mathbf{\Upsilon}(k)} = \frac{\partial J(k)}{\partial e(k)}\frac{\partial e(k)}{\hat{d}(k)}\frac{\partial\hat{d}(k)}{\partial\mathbf{\Upsilon}(k)}, \tag{15}$$

where another way to rewrite (15) is given by:

$$\frac{\partial J(k)}{\partial\mathbf{\Upsilon}(k)} = -e(k)\boldsymbol{\mathcal{X}}(k). \tag{16}$$

Through the chain rule, the partial derivative $\left(\dfrac{\partial}{\partial\mathbf{\Upsilon}(k)}\right)^v J(k)$ is given by [31]:

$$\left(\frac{\partial}{\partial\mathbf{\Upsilon}(k)}\right)^v J(k) = \frac{\partial J(k)}{\partial e(k)}\frac{\partial e(k)}{\partial\hat{d}(k)}\left(\frac{\partial}{\partial\mathbf{\Upsilon}(k)}\right)^v \hat{d}(k). \tag{17}$$

Definition 1 [31]: *The fractional derivative of Riemann-Liouville of a function f is given by:*

$$(D^v f)(t) = \frac{1}{\Gamma(k-v)}\left(\frac{d}{dt}\right)^v \int_0^{\mathrm{T}} (t-\tau)^{k-v-1}f(\tau)d\tau \tag{18}$$

$$(D^v f)(t-\alpha)^\alpha = \frac{\Gamma(1+\alpha)}{\Gamma(1+\alpha-v)}(t-\alpha)^{\alpha-v}, \tag{19}$$

where $1+\alpha-v > 0$, $t > 0$ and D is the differential operator. It is important to note that the gamma function $\Gamma(v)$ is defined as [32], [33]:

$$\Gamma(v) = \int_0^\infty t^{v-1}e^{-t}dt. \tag{20}$$

Using (16) and (19), (17) is rewritten as follows [29]:

$$\left(\frac{d}{d\mathbf{\Upsilon}(k)}\right)^v J(k) = -e(k)\boldsymbol{\mathcal{X}}(k)\frac{(\mathbf{\Upsilon}(k))^{1-v}}{\Gamma(2-v)}. \tag{21}$$

Substituting (16) and (21) into (14), it is obtained that:

$$\mathbf{\Upsilon}(k+1) = \mathbf{\Upsilon}(k) + \mu e(k)\boldsymbol{\mathcal{X}}(k) + \mu_f e(k)\boldsymbol{\mathcal{X}}(k)\frac{(\mathbf{\Upsilon}(k))^{1-v}}{\Gamma(2-v)}. \tag{22}$$

The equation of update of weight vector though MVSS-FLMS algorithm, according to [29], is obtained considering that $\mu_f = \mu\Gamma(2-f)$. Thus, (22) is rewritten as follows:

$$\begin{aligned} \mathbf{\Upsilon}(k+1) &= \mathbf{\Upsilon}(k) + \mu e(k)\boldsymbol{\mathcal{X}}(k) + \mu e(k)\boldsymbol{\mathcal{X}}(k)(\mathbf{\Upsilon}(k))^{1-v} \\ &= \mathbf{\Upsilon}(k) + \mu e(k)\boldsymbol{\mathcal{X}}(k)\left[1 + (\mathbf{\Upsilon}(k))^{1-v}\right] \end{aligned} \tag{23}$$

According to [29], it is important to note that the variable step size is obtained as follows:

$$\mu(k+1) = c\left[\mu(k)(0.1-\mu(k))\mathrm{exp}(-e(k)e(k-1))\right] \tag{24}$$

where $\mu(k)$ is the variable step size, c is a scaling parameter and $\mathrm{exp}(\bullet)$ is the exponential function. After obtained (24), (23) is rewritten as follows:

$$\mathbf{\Upsilon}(k+1) = \mathbf{\Upsilon}(k) + \mu(k)e(k)\boldsymbol{\mathcal{X}}(k)\left[1 + (\mathbf{\Upsilon}(k))^{1-v}\right] \tag{25}$$

IV. Computational Results

In this section, are presented the results obtained through DAIC design by the MVSS-FLMS algorithm and application to non-minimum phase plant referring to a system Electro-Hydraulic Actuator (EHA). The plant model $P(q^{-1})$ was obtained in [34], given by:

$$y(k) = \frac{-0.03093 + 0.3836q^{-1} - 0.2738q^{-2}}{1 - 1.57q^{-1} + 1.056q^{-2} - 0.1695q^{-3}}(u(k) + n(k)), \tag{26}$$

where $y(k)$ [mm] is the piston displacement of EHA system or plant output signal, $n(k)$ [V] is the disturbance signal added to the control signal $u(k)$ [V]. The plant model is stable with poles located at $0.6725 \pm 0.5488i$ and 0.2250. In addition, the plant model is non-minimum phase with zeros located at 11.6418 and 0.7604.

The results obtained through DAIC design by the MVSS-FLMS algorithm were compared with the results obtained through FLMS algorithm. For the FLMS algorithm, the value of the step sizes were set equal to $\mu = 5 \times 10^{-4}$, $\mu_f = 5 \times 10^{-4}$; the value of the fractional order was set equal to $v = 0.5$. For the MVSS-FLMS algorithm, the initial value of the step size was set equal to $\mu(1) = 5 \times 10^{-4}$ and the value of the fractional order was set equal to $v = 0.5$; the value of c in (24) was set equal to 0.01. The total time of simulation was set equal to 60 s, where the sampling period used was set equal to $T_s = 5$ ms.

The delay block q^{-L} was set with $L = 6$. In order to obtain non-conservative results, the reference signal $r(k) = A\mathrm{sin}(\omega t_s)$ is of sinusoidal type, where the frequency was set equal to 0.1Hz, $\omega = 2\pi f$, A is the maximum amplitude of

$r(k)$ and $t_s = T_s k$. It is important to note that at each 15 s the maximum amplitude of the reference signal $r(k)$ was changed, in the following sequence: 5 mm, 8 mm, 9 mm and 12 mm. The order of $\hat{C}(q^{-1})$ and $\hat{P}_{copy}(q^{-1}) = \hat{P}(q^{-1})$ was set equal to $M = N = 10$. In addition, it is important to note that the performance analysis of MVSS-FLMS and FLMS algorithms in DAIC design, in terms of convergence speed and steady-state MSE, was performed only for the controller $\hat{C}(q^{-1})$. The convergence speed of the weight vector $\mathbf{\Theta}(k)$ was analyzed through the convergence speed of $y(k)$ to $r(k)$. The steady-state MSE was analyzed through the error $e_c(k)$ used to update the estimate of the weight vector. In Fig. 2, it is shown the plant output signal $y(k)$. In Fig. 3, it is shown the disturbance signal $n(k)$. In Fig. 4, it is shown the reference error $e_{ref}(k)$.

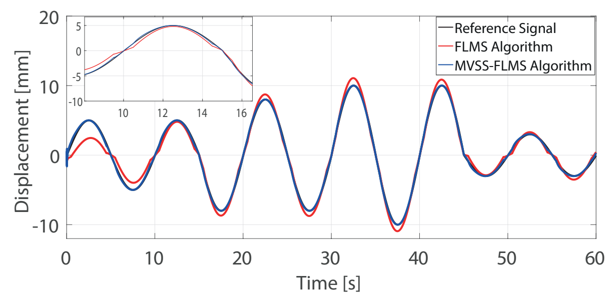

Fig. 2: Plant output signal $y(k)$ (obtained through DAIC designed by the FLMS and MVSS-FLMS algorithms) and reference signal $r(k)$.

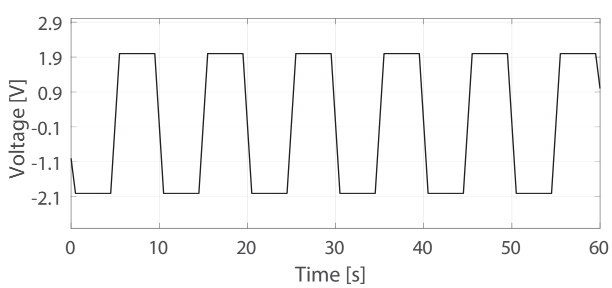

Fig. 3: Disturbance signal $n(k)$.

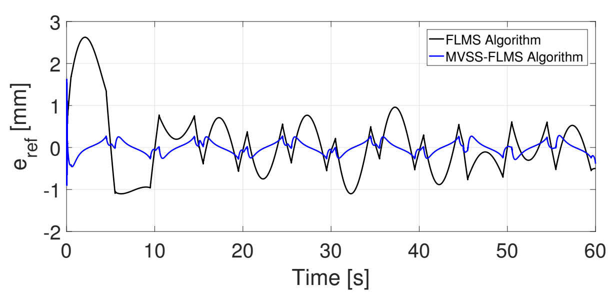

Fig. 4: Reference error $e_{ref}(k)$.

Due to the step size of MVSS-FLMS algorithm to be variable, even in the presence of the disturbance signal $n(k)$, a satisfactory tracking of the inverse plant dynamics was obtained through the update of the estimate of the weight vector $\mathbf{\Theta}(k)$ of the controller $\hat{C}(q^{-1})$. The satisfactory tracking of the inverse plant dynamics can be verified through the fast and satisfactory convergence of the plant output signal $y(k)$ to the reference signal $r(k)$, when compared to the FLMS algorithm. In addition, this result can be verified through the reference error, where it is possible to note that $e_{ref}(k)$ is smaller for the DAIC designed by the MVSS-FLMS algorithm, when compared to the FLMS algorithm. The estimation error $e_{mod}(k)$, used to update the estimate of the weight vector $\mathbf{\Pi}(k)$ of the model $\hat{P}(q^{-1})$, is shown in Fig. 5.

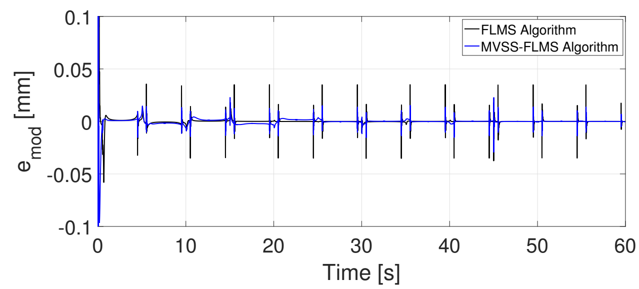

Fig. 5: Estimation error $e_{mod}(k)$.

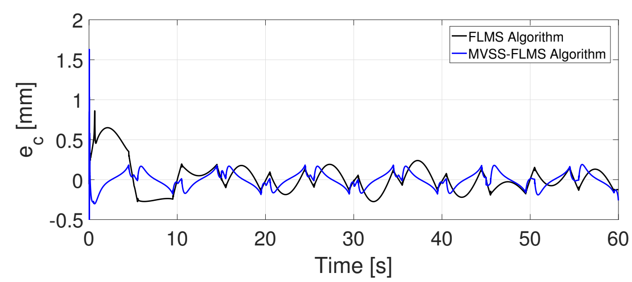

Fig. 6: Error $e_c(k)$.

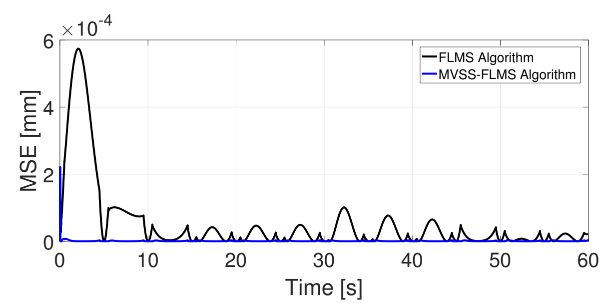

Fig. 7: MSE of $e_c(k)$.

In Fig. 6, it is shown the error $e_c(k)$, used to update the estimate of the weight vector $\mathbf{\Theta}(k)$ of the controller $\hat{C}(q^{-1})$. In Fig. 7, it is shown the MSE of $e_c(k)$. In Fig. 7, it is noted that the MSE of $e_c(k)$, for the DAIC designed by the MVSS-FLMS algorithm, quickly converges to zero, even in the presence of the disturbance signal. In Fig. 8, it is shown the control signal $u(k)$. It is possible to note that the control

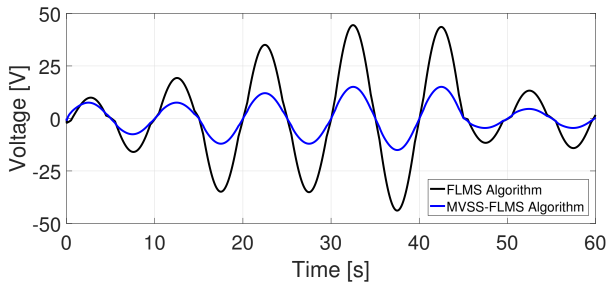

Fig. 8: Control signal $u(k)$.

signal $u(k)$ developed by the DAIC designed by the MVSS-FLMS algorithm obtained lower amplitudes when compared to the DAIC designed by the FLMS algorithm. The obtained results show that the update of the step size proposed by [29] allowed to the DAIC designed by the MVSS-LMS algorithm to obtain better results with respect to convergence speed and steady-state MSE, when compared to the DAIC designed by the FLMS algorithm.

V. Conclusion

In this work, it was performed the evaluation of performance of MVSS-FLMS algorithm in DAIC design applied to the control of non-minimum phase plant in the presence of disturbance signal added to the control signal. As presented, satisfactory results were obtained in terms of convergence speed and steady-state MSE for the MVSS-FLMS algorithm, confirmed through the satisfactory and fast convergence of $y(k)$ to $r(k)$ and steady-state MSE of $e_c(k)$ equal to zero, even in the presence of the disturbance signal.

References

[1] B. Widrow and E. Walach, "Adaptive signal processing for adaptive control," *IFAC Proceedings Volumes*, vol. 16, no. 9, pp. 7–12, 1983.

[2] K. Kuhnen and H. Janocha, "Adaptive inverse control of piezoelectric actuators with hysteresis operators," in *1999 European Control Conference (ECC)*. IEEE, 1999, pp. 791–796.

[3] J. L. Calvo-Rolle, O. Fontenla-Romero, B. Pérez-Sánchez, and B. Guijarro-Berdiñas, "Adaptive inverse control using an online learning algorithm for neural networks," *Informatica*, vol. 25, no. 3, pp. 401–414, 2014.

[4] A. Karshenas, M. Dunnigan, and B. Williams, "Adaptive inverse control algorithm for shock testing," *IEE Proceedings-Control Theory and Applications*, vol. 147, no. 3, pp. 267–276, 2000.

[5] T. Wang, S. Tong, J. Yi, and H. Li, "Adaptive inverse control of cable-driven parallel system based on type-2 fuzzy logic systems," *IEEE Transactions on Fuzzy Systems*, vol. 23, no. 5, pp. 1803–1816, 2014.

[6] X. F. Yuan, Y. N. Wang, and L. H. Wu, "Adaptive inverse control of excitation system with actuator uncertainty," *Neural processing letters*, vol. 27, no. 2, pp. 125–136, 2008.

[7] X. Zhang, Z. Li, C.-Y. Su, Y. Lin, and Y. Fu, "Implementable adaptive inverse control of hysteretic systems via output feedback with application to piezoelectric positioning stages," *IEEE Transactions on industrial electronics*, vol. 63, no. 9, pp. 5733–5743, 2016.

[8] G. Shen, S.-T. Zheng, Z.-M. Ye, Q.-T. Huang, D.-C. Cong, and J.-W. Han, "Adaptive inverse control of time waveform replication for electrohydraulic shaking table," *Journal of Vibration and Control*, vol. 17, no. 11, pp. 1611–1633, 2011.

[9] M. A. Shafiq, M. Shafiq, and N. Ahmed, "Closed loop direct adaptive inverse control for linear plants," *The Scientific World Journal*, vol. 2014, 2014.

[10] J. Yin, F. Dong, and N. Wang, "Direct adaptive inverse control based on variable radial basis function network," in *2006 6th World Congress on Intelligent Control and Automation*, vol. 1. IEEE, 2006, pp. 2709–2712.

[11] M. Shafiq, M. A. Shafiq, and H. A. Yousef, "Stability and convergence analysis of direct adaptive inverse control," *Complexity*, vol. 2017, 2017.

[12] B. Kamanditya and B. Kusumoputro, "Elman recurrent neural networks based direct inverse control for quadrotor attitude and altitude control," in *2020 International Conference on Intelligent Engineering and Management (ICIEM)*. IEEE, 2020, pp. 39–43.

[13] J. Gan and X. Zhang, "Adaptive control for piezoelectric actuator using direct inverse modeling approach," in *2016 International Conference on Manipulation, Automation and Robotics at Small Scales (MARSS)*. IEEE, 2016, pp. 1–5.

[14] B. Shoaib, I. M. Qureshi *et al.*, "Adaptive step-size modified fractional least mean square algorithm for chaotic time series prediction," *Chinese Physics B*, vol. 23, no. 5, p. 050503, 2014.

[15] R. Gorenflo and F. Mainardi, "Fractional calculus," in *Fractals and fractional calculus in continuum mechanics*. Springer, 1997, pp. 223–276.

[16] V. E. Tarasov, *Handbook of Fractional Calculus with Applications*. de Gruyter Berlin, Germany, 2019, vol. 5.

[17] R. Hilfer, *Applications of fractional calculus in physics*. World scientific, 2000.

[18] H.-P. Ren, X. Wang, J.-T. Fan, and O. Kaynak, "Fractional order sliding mode control of a pneumatic position servo system," *Journal of the Franklin Institute*, vol. 356, no. 12, pp. 6160–6174, 2019.

[19] N. I. Chaudhary, M. A. Z. Raja, J. A. Khan, and M. S. Aslam, "Identification of input nonlinear control autoregressive systems using fractional signal processing approach," *The Scientific World Journal*, vol. 2013, 2013.

[20] S. Khan, I. Naseem, M. A. Malik, R. Togneri, and M. Bennamoun, "A fractional gradient descent-based rbf neural network," *Circuits, Systems, and Signal Processing*, vol. 37, no. 12, pp. 5311–5332, 2018.

[21] N. I. Chaudhary, M. S. Aslam, D. Baleanu, and M. A. Z. Raja, "Design of sign fractional optimization paradigms for parameter estimation of nonlinear hammerstein systems," *Neural Computing and Applications*, vol. 32, no. 12, pp. 8381–8399, 2020.

[22] D. Yousri, A. M. AbdelAty, L. A. Said, A. Elwakil, B. Maundy, and A. G. Radwan, "Parameter identification of fractional-order chaotic systems using different meta-heuristic optimization algorithms," *Nonlinear Dynamics*, vol. 95, no. 3, pp. 2491–2542, 2019.

[23] J. Ahmad, S. Khan, M. Usman, I. Naseem, M. Moinuddin, and H. J. Syed, "Fclms: Fractional complex lms algorithm for complex system identification," in *2017 IEEE 13th International Colloquium on Signal Processing & its Applications (CSPA)*. IEEE, 2017, pp. 39–43.

[24] W. Song, M. Li, Y. Li, C. Cattani, and C.-H. Chi, "Fractional brownian motion: Difference iterative forecasting models," *Chaos, Solitons & Fractals*, vol. 123, pp. 347–355, 2019.

[25] B. Shoaib, I. M. Qureshi *et al.*, "A modified fractional least mean square algorithm for chaotic and nonstationary time series prediction," *Chinese Physics B*, vol. 23, no. 3, p. 030502, 2014.

[26] W. Dai, J. Huang, Y. Qin, B. Wang, and Y. Fang, "Regularity and classification of solutions to static hartree equations involving fractional laplacians," *Discrete & Continuous Dynamical Systems*, vol. 39, no. 3, p. 1389, 2019.

[27] A. Ahilan, G. Manogaran, C. Raja, S. Kadry, S. N. Kumar, C. A. Kumar, T. Jarin, S. Krishnamoorthy, P. M. Kumar, G. C. Babu *et al.*, "Segmentation by fractional order darwinian particle swarm optimization based multilevel thresholding and improved lossless prediction based compression algorithm for medical images," *Ieee Access*, vol. 7, pp. 89 570–89 580, 2019.

[28] R. M. A. Zahoor and I. M. Qureshi, "A modified least mean square algorithm using fractional derivative and its application to system identification," *European Journal of Scientific Research*, vol. 35, no. 1, pp. 14–21, 2009.

[29] Y. K. Barapatre, A. Patnaik, and S. Nanda, "A modified variable step size for fractional least mean square algorithm for system identification and its fpga implementation," in *2020 International Conference on Communication and Signal Processing (ICCSP)*. IEEE, 2020, pp. 1553–1558.

[30] P. S. Diniz *et al.*, *Adaptive filtering*. Springer, 1997, vol. 4.

[31] A. Atangana and J. Gómez-Aguilar, "Numerical approximation of riemann-liouville definition of fractional derivative: from riemann-

liouville to atangana-baleanu," *Numerical Methods for Partial Differential Equations*, vol. 34, no. 5, pp. 1502–1523, 2018.

[32] B. Ross, *Fractional calculus and its applications: proceedings of the international conference held at the University of New Haven, June 1974*. Springer, 2006, vol. 457.

[33] A. Loverro, "Fractional calculus: history, definitions and applications for the engineer," *Rapport technique, Univeristy of Notre Dame: Department of Aerospace and Mechanical Engineering*, pp. 1–28, 2004.

[34] R. Ghazali, Y. M. Sam, M. Rahmat, C. Soon, H. Jaafar *et al.*, "Discrete sliding mode control for a non-minimum phase electro-hydraulic actuator system," in *2015 10th Asian Control Conference (ASCC)*. IEEE, 2015, pp. 1–6.